SINTEF
PROCEEDINGS 6

14th International Conference on CFD in
Oil & Gas, Metallurgical and Process Industries
SINTEF, Trondheim, Norway, October 12–14, 2020

Proceedings from the 14th International Conference on CFD in Oil & Gas, Metallurgical and Process Industries

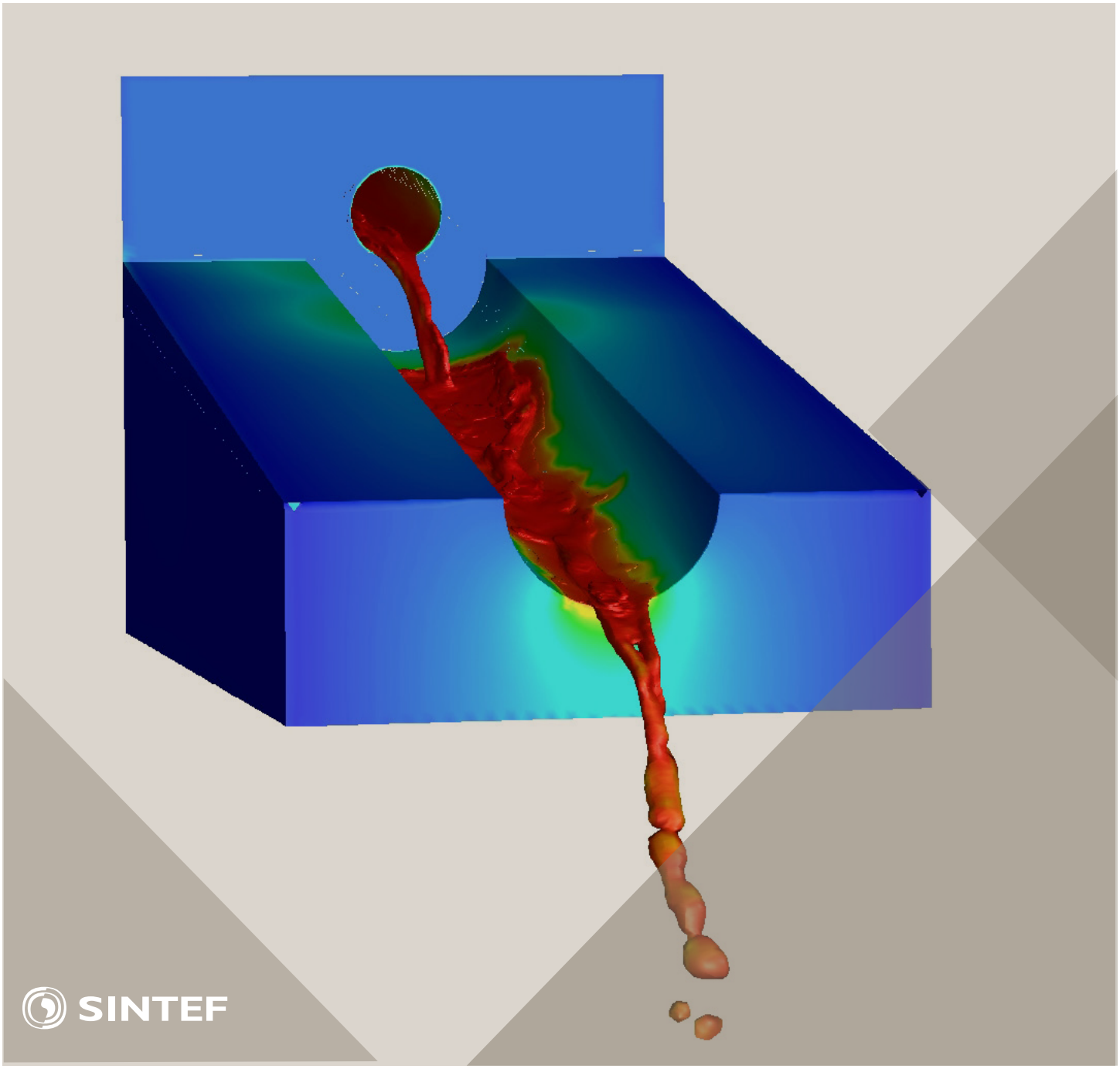

SINTEF Proceedings

Editors:
Jan Erik Olsen, Jan Hendrik Cloete and Stein Tore Johansen

Proceedings from the 14th International Conference on CFD in Oil & Gas, Metallurgical and Process Industries

SINTEF, Trondheim, Norway
October 12–14, 2020

SINTEF Academic Press

SINTEF Proceedings 6
Editors: Jan Erik Olsen, Jan Hendrik Cloete and Stein Tore Johansen

Proceedings from the 14th International Conference on CFD in Oil & Gas, Metallurgical and Process Industries, SINTEF, Trondheim, Norway, October 12–14, 2020

Keywords:
CFD, fluid dynamics, modelling

Cover illustration: Tapping of metal by Jan Erik Olsen

ISSN 2387-4295 (online)
ISBN 978-82-536-1684-1 (pdf)

SINTEF Academic Press
Address: Børrestuveien 3
PO Box 124 Blindern
N-0314 OSLO
Tel: +47 40 00 51 00

www.sintef.no/community
www.sintefbok.no

TO QUANTIFY MIXING QUALITY IN A SINGLE SCREW EXTRUDER SIMULATION

TJ Mateboer*, C Hummel, DJ van Dijk, J Buist

Windesheim University of Applied Sciences, Professorship for Polymer Engineering, P.O. Box 10090, 8000 GB Zwolle, The Netherlands

* E-mail: t.j.mateboer@windesheim.nl

ABSTRACT

Polymer mixing with a single screw extruder is a common process in industry. The mixing quality depends (amongst others) on the screw geometry. The main objective of this study was to develop a method for quantifying distributive mixing quality of a single screw extruder with computational fluid dynamics (CFD) simulations.
Tracer particles and Shannon entropy calculations were used to determine the distributive mixing quality as a function of direction, position in the extruder and scale of observation.
This method performed well for making a distinction in mixing quality between different extrusion simulations.

Keywords: CFD, Polymer mixing, distributive mixing, single screw extruder, Non-Newtonian fluid dynamics, Shannon entropy, Numerical simulation, spiral Maddock

NOMENCLATURE

Greek Symbols

$\dot{\gamma}$	Shear rate, [s^{-1}].
η	Viscosity, [Pa·s].
η_0	Viscosity at zero shear rate, [Pa·s].
η_∞	Viscosity at infinite shear rate, [Pa·s].
λ	Relaxation time, [s].
τ	Shear stress, [Pa].

Latin Symbols

c_i	Number of particles in bin *i*, [-].
i	Bin number, [-].
$\mathcal{M}$	Number of bins, [-].
m	Flow consistency index, [Pa·s^n].
N	Total number of tracer particles, [-].
n	Power law index, [-].
p_i	Probability of a particle to flow through bin *i*.
S_{rel}	Relative Shannon entropy, [-].

INTRODUCTION

Polymer mixing with a single screw extruder is a common process in industry. Mixing quality is often divided into dispersive and distributive mixing. With distributive mixing the additive units or the discontinuous phase are/is homogeneously distributed throughout the polymer. Mixing quality depends on (amongst others) the screw geometry. Specialized mixing sections in a screw geometry are necessary for a high mixing quality with a single screw extruder. The spiral Maddock is such a mixing section.

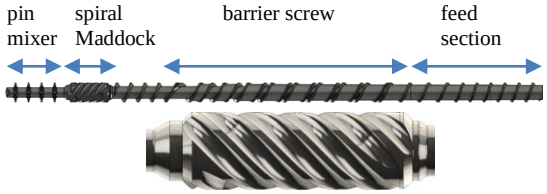

Figure 1: Upper: Extruder screw with four section. Fluid flow is from right to left. Lower: spiral Maddock section.

With computational fluid dynamics (CFD) many different mixing parameters can be simulated, such as different screw geometries. A more efficient mixer may be found by comparing several simulated extruders. Mixing quality has to be quantified in order to find the best mixer. The goal of this study was to find a method of quantifying mixing quality in a single screw extruder using CFD simulation.
Several studies have modeled polymer mixing with CFD (1-13). Distributive mixing behavior in simulations is often quantified with a residence time distribution (RTD) of tracer particles (1, 5, 14-18) and with the Shannon entropy (6, 8, 15, 16, 19, 20). These methods often result in limited information of:

- Mixing quality in different directions (angular and radial directions separately).
- Mixing quality at different positions in the extruder.
- Mixing quality at both a large and small scale of observation.

In this study a method was developed applying the Shannon entropy for calculating distributive mixing quality as function of the position in the extruder, as function of direction and scale. For several extrusion simulations the mixing quality was calculated to determine how well a distinction in mixing quality can be made with this method. These extrusion simulations were only used to test the method of quantifying mixing quality, the study is not focused on finding an optimized

screw geometry. Furthermore only the spiral Maddock screw mixing section was included in the simulations, not the whole extruder.

SIMULATION SETUP

To show the effectiveness of the method extrusion simulations with the spiral Maddock were performed. The flight height and the rotational velocity was varied between the simulations. The specifics of the simulations are shown in this section. The simulations were performed with the immersed solid method (ISM) in CFX (Ansys 19.2). All the simulations are steady state and isothermal.

Spiral Maddock geometry

The spiral Maddock is a mixing section of a single screw extruder with a 75 mm diameter, see Figure 1. The spiral Maddock is specifically designed for dispersive mixing, while in this study only distributive mixing quality was calculated. The simulations were created in order to have a data set to test the method for determining mixing quality. Therefore the exact purpose of the screw section was not significant for this study. The spiral Maddock consist of several flights, inflow and outflow channels. The spiral Maddock is discrete rotational sy[illegible]ng th[illegible]xis.

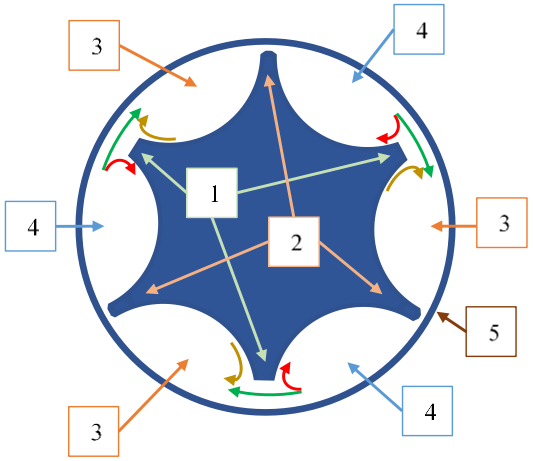

Figure 2: Schematic cross section of a spiral Maddock. 1: barrier flights. 2: main flights. 3: outflow channels. 4: inflow channels. 5: barrel.

The spiral Maddock is designed in such a way that the fluid passes through a gap between the barrier flight and the barrel. The barrier flight height was varied so the gap between the barrier flight and the barrel was varied between 1.74 mm and 0.74 mm.
The gap between the main flight and the barrel wall is very narrow in order to prevent fluid flowing through. The size of this gap makes meshing difficult. Therefore the main flight was extended beyond the barrel wall. With this setup the gap between the main flight and the barrel wall does not exist in the simulations. This simplification of the model was expected to have minor effects on outcome of this study. This is justified since the simulations were used to create a dataset for applying the method to determine mixing quality.

Boundary conditions

A no slip condition was set on both the barrel and screw walls. The screw rotates relative to the barrel wall. The mass flow rate condition was set to $20 \cdot 10^{-6}$ m^3s^{-1}. At the outflow opening the pressure was set to 0 Pa.

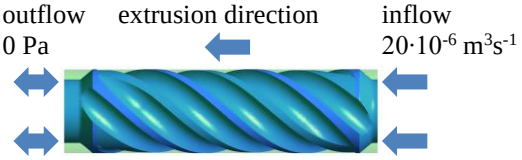

Figure 3: Side view of the spiral Maddock. The screw is in blue, the fluid domain is in green.

Simulations were performed with a screw rotational velocity of both 1.5 rad/s and 4.6 rad/s.

Material parameters

The input of the material parameters were derived from an HDPE grade (Marlex TRB-432, Chevron Phillips Chemical Company). The viscosity as function of shear rate was determined with a capillary rheometer at 200 °C. Measurements were performed in a shear rate range from $\dot{\gamma} = 4\,s^{-1}$ up to $\dot{\gamma} = 500\,s^{-1}$. A power law was fitted onto the rheological measurements with n = 0.35 and m = $3.3 \cdot 10^4$ $Pa \cdot s^{-n}$.
Power law

$$\tau = m\dot{\gamma}^n \qquad (1)$$

For numerical stability a Bird-Carreau model was used in the simulations:
Bird-Carreau model

$$\eta = \eta_\infty + (\eta_0 - \eta_\infty)\left(1 + (\lambda\dot{\gamma})^2\right)^{\frac{n-1}{2}} \qquad (2)$$

The Bird-Carreau and the power law are almost identical in the shear rate range of $\lambda^{-1} > \dot{\gamma} > \left(\frac{\eta_\infty}{m}\right)^{\frac{1}{n-1}}$. λ and η_∞ were chosen in such a way that the power law and the Bird-Carreau are similar behavior at $10^{-3} > \dot{\gamma} > 10^7$. The chosen values were η_∞ = 1 Pa·s, η_0 = 3 MPa·s and λ = 1000 s. These values were chosen since lower and higher shear rates were not expected to have a significant influence on the simulation. Furthermore no rheological measurements were available at those low and high shear rates.

Mesh

A fluid domain and an immersed solid were created.

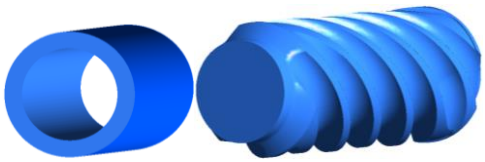

Figure 4: Left: fluid domain. Right: immersed solid domain (spiral Maddock).

The two domains were meshed separately. The fluid domain mesh consists of a part with cubical cells near the barrel wall.

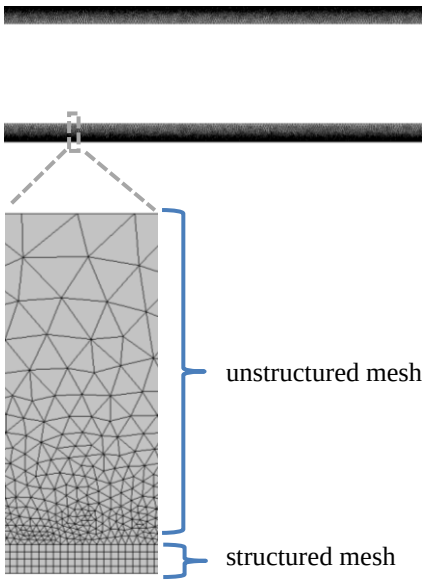

Figure 5: Cross section of a fluid domain mesh.

The height of this structured part is similar in size to the gap between the barrier flight and the barrel. This ensures a minimum number of cells between the barrier flight and the barrel wall. A large aspect ratio in these cells resulted in numerical instabilities, therefore the structured cells are cubical.
The rest of the fluid domain consists of an unstructured mesh. The results of a simulation with a proper mesh density do not change when the mesh cell density is increased. The cell size of the cubical cells was incrementally reduced from an average cell size of 0.15 mm down to 0.05 mm. The unstructured cell was reduced in size accordingly. The total number of cells increased from 58 M up to 479 M.
Simulations with the different meshes were evaluated by comparing the pressure at the inflow of the spiral Maddock.
The immersed screw mesh size does not have a great impact on the computational costs. Therefore a single fine mesh was made of the screw. This unstructured mesh was used in each of the simulations.

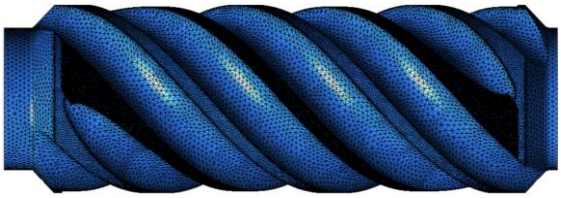

Figure 6: Side view of the immersed solid domain mesh / screw mesh.

It is preferred to have a well-defined gap between the barrel and the barrier flight. Therefore a very fine mesh was chosen for the barrier flight back.

Tracer particles

The flow paths of the fluid determine the quality of the distributive mixing. The flow paths can be determined with tracer particles of zero mass (21). These flow paths were calculated in a post processor (Ansys CFD-Post) with the streamline function. The flow paths consists of a series of points. The fluid velocity and trajectory at a point can be used to calculate the position of the next point. The distance between the points is a factor of 0.01 of the mesh cell size. Therefore a smaller cell size results in more accurate tracer particle path.
In total 10^5 tracer particles were introduced at the inflow boundary. The position of the inflow boundary is shown in Figure 3.

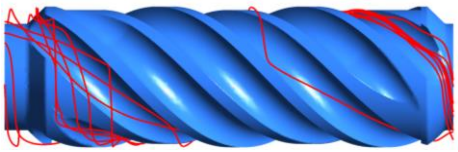

Figure 7: Example of the trajectory of a small number of tracer particles introduced at the inflow boundary into the spiral Maddock simulation.

The particle inflow positions, and a method to determine mixing quality is shown in the next section.

Variation in the simulation setup

3 different simulations were executed. The configurations are shown in Table 1.

Table 1: Modelling conditions.

simulation name	screw rotational velocity	Gap between the barrier flight and the barrel
standard	1.5 rad/s	0.74 mm
high screw velocity	4.6 rad/s	0.74 mm
lowered barrier flight	1.5 rad/s	1.74 mm

The standard setup was used for the mesh study. The mixing quality was calculated for all three setups. The purpose of the different setups was to determine how well a distinction in mixing quality can be made with the Shannon entropy. The setups were not chosen to determine an optimal extrusion setup or screw geometry.

SHANNON ENTROPY FOR DETERMINING THE MIXING QUALITY

Shannon entropy is a single measure to determine a distribution across a number of bins (M). Relative Shannon entropy (S_{rel}) is calculated with the probability (p_i) that a tracer particle flows through a bin and will be referred to from here on as the Shannon entropy.
Relative Shannon entropy

$$S_{rel} = \frac{-\sum_{i=1}^{M} p_i \ln p_i}{\ln M} \qquad (3)$$

p_i is equal to the number of tracers (c_i) in bin i divided by the total number of tracer particles (N).
The Shannon entropy was calculated at the outflow side of the spiral Maddock, see Figure 3. Therefore the outflow was divided into several bins, see the example in Figure 8.

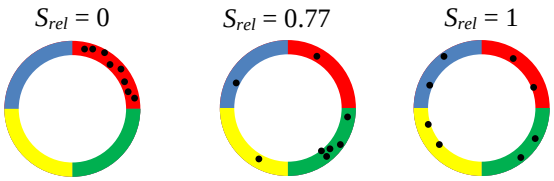

Figure 8: Outflow divided into 4 bins with eight tracer particles. Left low quality mix (S_{rel} = 0), middle: medium quality mix (S_{rel} = 0.77), right: high quality mix (S_{rel} = 1).

The mixing quality is low with a inhomogeneous probability distribution, see the particle distribution in the most left outflow in Figure 8. The mixing quality is high with a homogeneous probability distribution, see the particle distribution in the most right outflow in Figure 8. The Shannon entropy is a measure of probability distribution, therefore the Shannon entropy can be applied as a measure of mixing quality.
A low Relative Shannon entropy corresponds to a low mixing quality. The maximum Relative Shannon entropy and maximum mixing quality is reached when S_{rel} = 1. The Relative Shannon entropy is in the range $0 < S_{rel} \leq 1$, which makes it possible to estimate the mixing quality with the Relative Shannon entropy.
It seems reasonable that a lower number of particles per bin results in an increase in uncertainty in the Shannon entropy. Therefore the average number of particles per bin was kept at a minimum of 30 particles. All the Shannon entropy calculation were performed with GNU Octave.

Bin division schemes

The orientation of the bin division scheme determines the direction of mixing quality that can be calculated with the Shannon entropy. Mixing quality in an angular direction (angular mixing quality) can be calculated with an angular bin division scheme. Mixing quality in a radial direction (radial mixing quality) has to be calculated with a radial bin division scheme.

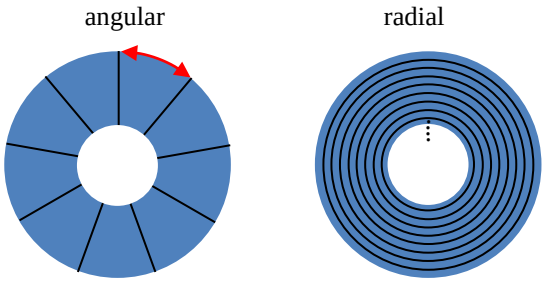

Figure 9: Schematic of bin distribution schemes. Left: angular divisions, the red arrow indicates the typical size for this bin division. Right: radial division.

The above schematic shows two bin division with 8 bins. The typical size of the angular bins is the circumference divided by the number of bins (M), see the red arrow in the above figure. The typical size of the radial bins is the distance between the screw and the barrel divided by the number of bins (M). The bin size defines the scale of observation (6). Mixing quality at a macroscopic level can be determined with a small number of bins. Mixing quality on a microscopic level needs to be determined with a large number of bins. From 3 up to 96 bins were used to calculate a Shannon entropy.

Tracer particle inflow sections

The tracer particles flow from the inflow boundary to the outflow boundary, see Figure 3. The increase in homogeneity of the particle distribution represents the increase in mixing quality. Therefore it is preferred to have a inhomogeneous particle distribution at the inflow. The particles were grouped together in a section of the inflow boundary, see Figure 10.

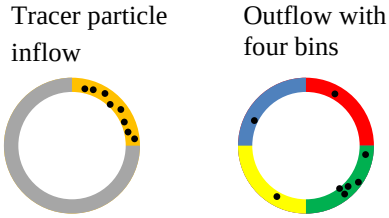

Figure 10: Left: an inflow boundary with, in orange, a section were 8 particles were introduced. Right: an outflow boundary divided into 4 bins.

An inflow sections, such as shown in Figure 10, has the same size and shape as an outflow bin. If there is no mixing in the simulation, than all the particle would end up in 1 bin at the outflow. And the Shannon entropy would be S_{rel} = 0.
Mixing quality as function of position at the inflow can be determined by using several inflow section with different sets of particles. The Shannon entropy can be calculated for each inflow section independently.

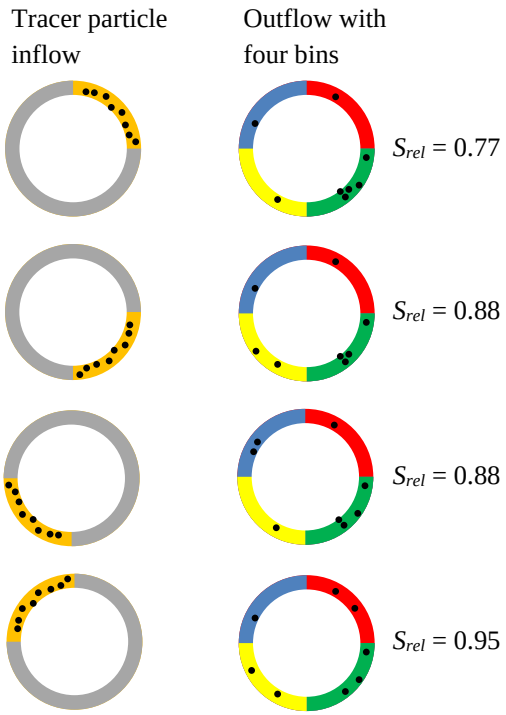

Figure 11: A hypothetical example of four Shannon entropy calculations based on an angular bin division scheme and different section for particle entry.

Figure 11 shows an example for an angular bin division scheme with 4 separate bins. The inflow sections are the same size as the bins, therefore the inflow (in the

example) is divided into 4 section. A different Shannon entropy can be calculated for each inflow section. Multiple inflow sections can also be used with a radial bin division scheme. In that case the inflow is divided in a radial direction. With this method the Shannon entropy as a function of inflow position (angular and radial) can be calculated.
The spiral Maddock consists of 3 rotational symmetric parts, see Figure 2. The Shannon entropy as function of inflow position is also expected to be symmetrical. Therefore only 1/3 of the inflow is divided into section with particles.

RESULTS

Mesh study

Simulations with the different meshes were compared based on pressure at the inflow of the spiral Maddock.

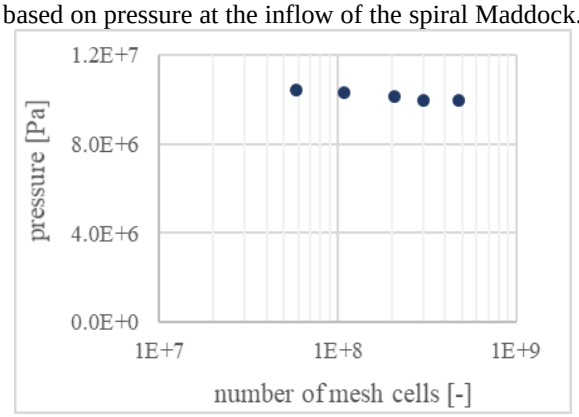

Figure 12: Simulated pressure at the inflow of the spiral Maddock as function of mesh size.

The pressure does not reduce much with increase of mesh size. As can be seen from Figure 12, a limited reduction of the pressure was calculated with increasing mesh size. Therefore the most coarse mesh (58 M cells) was used to determine mixing quality.

Particle distribution

In the next step tracer particles were introduced to determine mix quality. An example of the particle positions at the outflow boundary is shown in Figure 13. In this example the particles were introduced at a section of 1/3 of the inflow boundary. The outflow was divided into 3 bins in an angular direction.

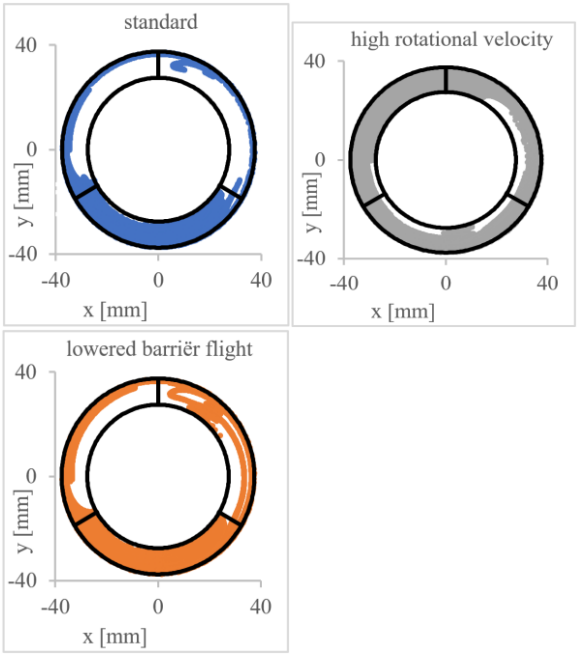

Figure 13: Tracer particle positions (colored dots) at the outflow of the spiral Maddock. The outflow is divided into 3 bins.

The figure allows for a visual evaluation of the mixing quality. The simulation with a high rotational screw velocity shows (visually) a higher mixing quality compared to the other simulations. The standard and lowered barrier flight show a very similar particle distribution.
The outflow was divided, in an angular direction, in 3 bins for the Shannon entropy calculations. The bins were large with a typical size of 79 mm (in angular direction, see Figure 9). The Shannon entropy is 0.95 for the simulation with a high rotational screw velocity, S_{rel} = 0.68 for the lowered flight simulation, and S_{rel} = 0.56 for the standard simulation. A high Shannon entropy corresponds to a high distributive mixing quality in angular direction. Therefore the simulation with a high screw velocity is the better mixer for mixing in angular direction at this large scale (typical bin size is 79 mm).

Angular distributive mixing quality

The mixing quality was visually evaluated in the above paragraph, and quantified for 1 inflow section at 1 scale of observation. This section shows the quantified mixing quality for several scales of observation and several positions at the inflow.
The inflow of the spiral Maddock was divided into sections in an angular direction. The tracer particles were introduced in each section and the Shannon entropy was calculated for each section. Figure 14 shows the Shannon entropy as function of inflow section with an angular bin division scheme.

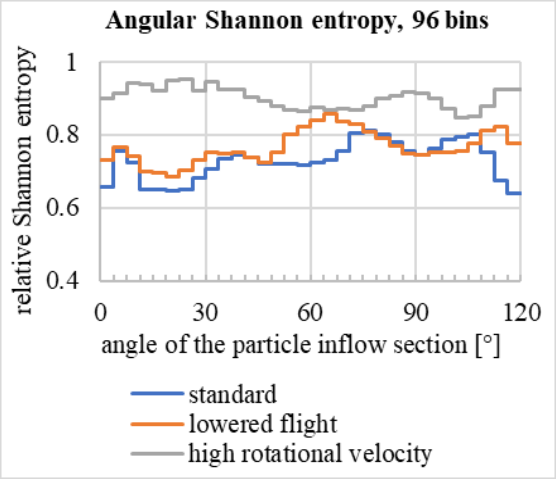

Figure 14: Shannon entropy as a function of inflow section with an angular bin division scheme and a typical bin size of 2.5 mm.

A high Shannon entropy corresponds to a high distributive mixing quality while a low Shannon entropy corresponds to a low distributive mixing quality. The angular mixing quality depends on the tracer particle inflow section. For example the lowered flight simulation: the mixing quality is better for inflow section at 60.75°-67.50° (S_{rel} = 0.86) while the mixing quality is less (S_{rel} = 0.73) for the inflow section at 0°-3.75°. The high rotational velocity shows a higher mixing quality. Figure 14 only shows the results with a typical bin width of 2.5 mm. A minimum or an average mixing quality of all inflow section can be used to show mixing quality at other scales of observation.

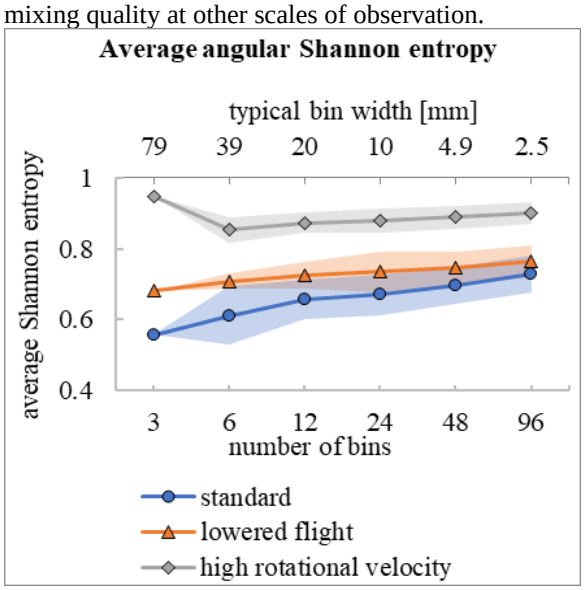

Figure 15: Average angular Shannon entropy as an function of the number of bins (bottom axis) and typical bin width (top axis). The colored bands show the standard deviation. Note: the horizontal axis is on a logarithmic scale.

The high rotational velocity simulation shows a higher average Shannon entropy compared to the other simulations. And therefore the high rotational velocity shows a higher distributive mixing quality. The lowered flight simulation shows a slightly higher average angular mixing quality compared to the standard simulation at each typical bin width. Although there is a certain overlap when the standard deviation is taken into account. The mixing quality of the simulations can also be compared with the minimum Shannon entropy of a simulation at a specific typical bin width.

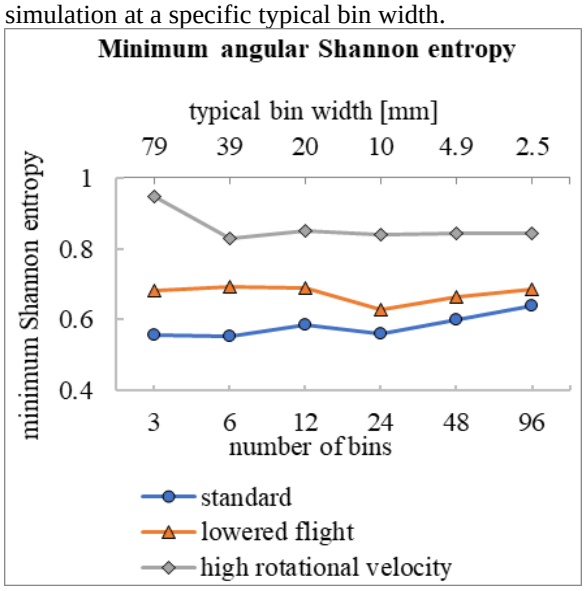

Figure 16: Minimum angular Shannon entropy as function of number of bins (bottom axis) and typical bin width (top axis). The colored bands show the standard deviation. Note: the horizontal axis is on a logarithmic scale.

Comparing the minimum Shannon entropy is useful for a design study when a minimum mixing quality is required. The lowest angular mixing quality of the lowered flight simulation is better than the lowest mixing quality of the standard simulation at all typical bin widths.
The Shannon entropy can be used to make a distinction in angular mixing quality between the extrusion simulations. Furthermore the angular mixing quality was determined as function of angular position and of scale of observation.

Radial distributive mixing quality

Shannon entropy was calculated with a radial bin division scheme. The inflow was divided into radial sections. Figure 17 shows the Shannon entropy as a function of radial inflow section.

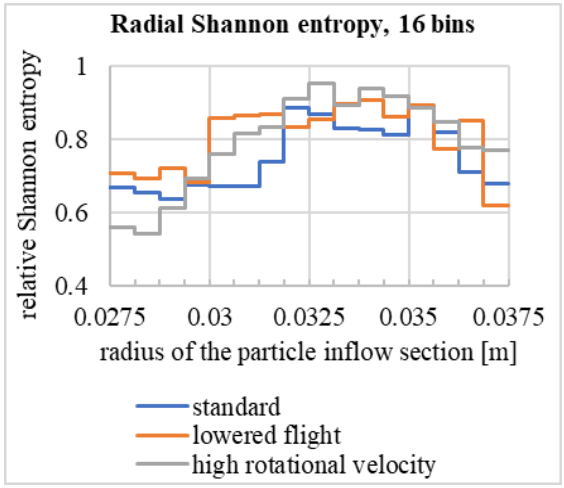

Figure 17: Shannon entropy as a function of inflow section with a radial bin division scheme and a typical bin size of 0.6 mm.

It was found that the distributive mixing quality in the radial direction depends on the radial position of the particle inflow section. The mixing quality shows a dependency on the inflow position rather than on the simulation setups included in this study. Therefore it is not meaningful to compare the average or minimum Shannon entropy as was performed with the angular bin distribution.

CONCLUSION AND RECOMMENDATIONS

With this method tracer particles and Shannon entropy calculations were used to determine the distributive mixing quality as function of:

- radial and angular direction
- scale of observation
- radial and angular inflow position of the tracer particles

For 3 spiral Maddock simulations the mixing quality was calculated to determine how well a distinction in mixing quality can be made with this method. The flight height and the rotational velocity was varied in these simulation. The mixing quality depends on both the angular and radial inflow position of the tracer particles. The different simulations show different mixing quality in angular direction. Therefore this method can be applied to determine which extruder the most efficient angular mixer is.

Recommendation / future work

In this study only a single mixing section of an extruder was included (the spiral Maddock) and the simulations were not verified with experiments. Future work will focus on including the whole screw and the extruder die and verifying the simulations with experiments, specifically the distributive mixing quality of the simulations.

ACKNOWLEDGEMENTS

This study was financially supported by Tech For Future (TFF) and Wavin T&I. The Windesheim University Professorship for Polymer Engineering conducted this study with Wavin T&I. Wavin T&I provided expert advice, essential equipment, materials and experimental data.

REFERENCES

1. Zong Y, Tang H, Zhao L. 3-D numerical simulations for polycondensation of poly(p-phenylene terephthalamide) in twin screw extruder. Polymer Engineering and Science. 2017;57(11):1252-61.
2. Tang H, Zong Y, Zhao L. Numerical simulation of micromixing effect on the reactive flow in a co-rotating twin screw extruder. Chinese Journal of Chemical Engineering. 2016;24(9):1135-46.
3. Zhang XM, Xu ZB, Feng LF, Song XB, Hu GH. Assessing local residence time distributions in screw extruders through a new in-line measurement instrument. Polymer Engineering & Science. 2006;46(4):510-9.
4. Zhang XM, Feng LF, Hoppe S, Hu GH. Local residence time, residence revolution, and residence volume distributions in twin-screw extruders. Polymer Engineering & Science. 2008;48(1):19-28.
5. Zhang XM, Feng LF, Chen WX, Hu GH. Numerical simulation and experimental validation of mixing performance of kneading discs in a twin screw extruder. Polymer Engineering & Science. 2009;49(9):1772-83.
6. Manas-Zloczower I, Kaufman M, Alemaskin K, Camesasca M. Color Mixing in Extrusion: Simulations and Experimental Validation. NSF DMII Grantees Conference; Scottsdale Arizona, USA2005.
7. Alemaskin K, Manas-Zloczower I, Kaufman M. Color mixing in the metering zone of a single screw extruder: numerical simulations and experimental validation. Polymer Engineering & Science. 2005;45(7):1011-20.
8. Alemaskin K, Manas-Zloczower I, Kaufman M. Entropic analysis of color homogeneity. Polymer Engineering & Science. 2005;45(7):1031-8.
9. Alemaskin K. Entropic Measures of Mixing in Application to Polymer Processing: Case Western Reserve University; 2004.
10. Alemaskin K, Camesasca M, Manas-Zloczower I, Kaufman M, editors. Entropic measures of mixing tailored for various applications. AIP Conference Proceedings; 2004: AIP.
11. Alemaskin K, Camesasca M, Manas-Zloczower I, Kaufman M, Kim E, Spalding MA, et al., editors. Entropic mixing characterization in a single screw extruder. SPE ANTEC; 2004.
12. Alemaskin K, Manas–Zloczowe I, Kaufman M. Index for simultaneous dispersive and distributive mixing characterization in processing equipment. International Polymer Processing. 2004;19(4):327-34.
13. Alemaskin K, Manas-Zloczower I, Kaufman M, editors. Simultaneous characterization of dispersive and distributive mixing in a single screw extruder. Proceedings of the Int Conf ANTEC; 2003.
14. Wang W, Zloczower I, editors. Dispersive and distributive mixing characterization in extrusion equipment. Antec 2001 Conference Proceedings; 2001.
15. Tadmor Z, Gogos CG. Principles of Polymer Processing: Wiley; 2006.
16. Xu B, Yu H, Kuang T, Turng LS. Evaluation of Mixing Performance in Baffled Screw Channel Using Lagrangian Particle Calculations. Advances in Polymer Technology. 2017;36(1):86-97.
17. Yamada S, Fukutani K, Yamaguchi K, Funahashi H, Ebata K, Uematsu H, et al. Dispersive mixing performance evaluation of special rotor segments in an intermeshing co-rotating twin-screw extruder by using weighted probability distributions. International Polymer Processing. 2015;30(4):451-9.
18. Chen J, Cao Y, editors. Simulation of 3D flow field of RPVC in twin-screw extrusion under wall slip conditions. Proceedings of 2012 9th International Bhurban Conference on Applied Sciences and Technology, IBCAST 2012; 2012.
19. Wang W, Manas-Zloczower I, Kaufman M. Entropic characterization of distributive mixing in polymer processing equipment. AIChE Journal. 2003;49(7):1637-44.
20. Manas-Zloczower I, Agassant JF. Mixing and Compounding of Polymers: Theory and Practice: Hanser; 2009.
21. Ansys C-P. CFD-Post User's Guide. Ansys Inc.